Pattern Recognition 44 (2011) 1–15

Contents lists available at ScienceDirect

Pattern Recognition

journal homepage: www.elsevier.com/locate/pr

Color image segmentation using histogram thresholding – Fuzzy C-means hybrid approach

Khang Siang Tan, Nor Ashidi Mat Isa*

Imaging and Intelligent Systems Research Team (ISRT), School of Electrical and Electronic Engineering, Engineering Campus, Universiti Sains Malaysia, 14300 Nibong Tebal, Penang, Malaysia

ARTICLE INFO

Article history:
Received 29 March 2010
Received in revised form
2 July 2010
Accepted 4 July 2010

Keywords:
Color image segmentation
Histogram thresholding
Fuzzy C-means

ABSTRACT

This paper presents a novel histogram thresholding – fuzzy C-means hybrid (HTFCM) approach that could find different application in pattern recognition as well as in computer vision, particularly in color image segmentation. The proposed approach applies the histogram thresholding technique to obtain all possible uniform regions in the color image. Then, the Fuzzy C-means (FCM) algorithm is utilized to improve the compactness of the clusters forming these uniform regions. Experimental results have demonstrated that the low complexity of the proposed HTFCM approach could obtain better cluster quality and segmentation results than other segmentation approaches that employing ant colony algorithm.

1. Introduction

Color is one of the most significant low-level features that can be used to extract homogeneous regions that are most of the time related to objects or part of objects [1–3]. In a 24-bit true color image, the number of unique colors usually exceeds half of the image size and can reach up to 16 millions. Most of these colors are perceptually close and cannot be differentiated by human eye that can only internally identify a number of 30 colors in cognitive space [4,5]. For all unique colors that perceptually close, they can be combined to form homogeneous regions representing the objects in the image and thus, the image could become more meaningful and easier to be analyzed. In image processing and computer vision, color image segmentation is a central task for image analysis and pattern recognition [6–23] It is a process of partitioning an image into multiple regions that are homogeneous with respect to one or more characteristics.

Although many segmentation techniques have been appeared in scientific literature, they can be divided into image-domain based, physics based and feature-space based techniques [24]. These segmentation techniques have been used extensively but each has its own advantages and limitations. Image-domain based techniques utilize both color features and spatial relationship among color in its homogeneity evaluation to perform segmentation. These techniques produce the regions that have reasonable compactness of regions but facing difficulty in the selection of suitable seed regions. Physics based techniques utilize the physical models of the reflection properties of material to carry out color segmentation but more application specific, as they model the causes that may produce color variation. Feature-based techniques utilize color features as the key and the only criteria to segment image. The segmented regions are usually fragmented since the spatial relationship among color is ignored [25]. But this limitation can be solved by improving the compactness of the regions.

In computer vision and pattern recognition, Fuzzy C-means (FCM) algorithm has been used extensively to improve the compactness of the regions due to its clustering validity and simplicity of implementation. It is a pixels clustering process of dividing pixels into clusters so that pixels in the same cluster are as similar as possible and those in different clusters are as dissimilar as possible. This accords with segmentation application since different regions should be visually as different as possible. However, its implementation often encounters two unavoidable initialization difficulties of deciding the cluster number and obtaining the initial cluster centroids that are properly distributed. These initialization difficulties have their impacts on segmentation quality. While the difficulty of deciding the cluster number could affect the segmented area and region tolerance for feature variance, the difficulty of obtaining the initial cluster centroids could affect the cluster compactness and classification accuracy.

Recently, some feature-based segmentation techniques have employed the concept of ant colony algorithm (ACA) to carry out image segmentation. Due to the intelligent searching ability of the

* Corresponding author. Tel.: +60 45996093; fax: +60 45941023.
E-mail addresses: khangsiang85@hotmail.com (K. Siang Tan), ashidi@eng.usm.my (N.A. Mat Isa).

0031-3203/$ - see front matter © 2010 Elsevier Ltd. All rights reserved.
doi:10.1016/j.patcog.2010.07.013

ACA, these techniques could achieve further optimization of segmentation results. But they are suffering from low efficiency due to their computational complexity. Apart from obtaining good segmentation result, the improved ant system algorithm (AS) as proposed in [26] could also provide a solution to overcome the FCM's sensitiveness to the initialization condition of cluster centroids and centroid number. However, the AS technique does not seek for very compact clustering result in the feature space. To improve the performance of the AS, the ant colony – Fuzzy C-means hybrid algorithm (AFHA) is introduced [26]. Essentially, the AFHA incorporates the FCM algorithm to the AS in order to improve the compactness of the clustering results in the feature space. However, its efficiency is still low due to computational complexity of the AS. To increase the algorithmic efficiency of the AFHA, the improved ant colony – Fuzzy C-means hybrid algorithm (IAFHA) is introduced [26]. The IAFHA adds an ant sub-sampling based method to modify the AFHA in order to reduce its computational complexity thus has higher efficiency. Although the IAFHA's efficiency has been increased, it still suffers from high computational complexity.

In this paper, we propose a novel segmentation approach called Histogram Thresholding – Fuzzy C-means Hybrid (HTFCM) algorithm. The HTFCM consists of two modules, namely the histogram thresholding module and the FCM module. The histogram thresholding module is used for obtaining the FCM's initialization condition of cluster centroids and centroid number. The implementation of this module does not require high computational complexity comparing to those techniques using ant system. This marked the simplicity of the proposed algorithm.

The rest of the paper is organized as follows: Section 2 presents the histogram thresholding module and the FCM module in detail. Section 3 provides the illustration of the implementation procedure. Section 4 analyzes the result obtained for the proposed approach and at the same time comparing it to other techniques. Finally, Section 5 concludes the work of this paper.

2. Proposed approach

In this paper, we attempt to obtain a solution to overcome the FCM's sensitiveness to the initialization conditions of cluster centroid and centroid number. The histogram thresholding module is introduced to initialize the FCM in view of the drawbacks by taking the global information of the image into consideration. In this module, the global information of the image is used to obtain all possible uniform regions in the image and thus the cluster centroids and centroid number could also be obtained. The FCM module is then used to improve the compactness of the clusters. In this context, the compactness refers to obtaining the optimized label for each cluster centroid from the members of each cluster.

2.1. Histogram thresholding

Global histogram of a digital image is a popular tool for real-time image processing due to its simplicity in implementation. It serves as an important basis of statistical approaches in image processing by producing the global description of the image's information [27]. For color images with RGB representation, the color of a pixel is a mixture of the three primitive colors red, green and blue. Each image pixel can be viewed as three dimensional vector containing three components representing the three colors of an image pixel. Hence, the global histograms representing three primitive components, respectively, could produce the global information about the entire image.

The basic analysis approach of global histogram is that a uniform region tends to form a dominating peak in the corresponding histogram. For a color image, a uniform region could be identified by the dominating peaks in the global histograms. Thus, histogram thresholding is a popular segmentation technique that looks for the peaks and valleys in histogram [28,29]. A typical segmentation approach based on histogram analysis can only be carried out if the dominating peaks in the histogram can be recognized correctly. Several widely used peak-finding algorithms examined the peak's sharpness or area to identify the dominating peaks in the histogram. Although these peak-finding algorithms are useful in histogram analysis, they sometimes do not work well especially if the image contains noise or radical variation [30,31].

In this paper, we propose a novel histogram thresholding technique containing three phases such as the peak finding technique, the region initialization and the merging process. The histogram thresholding technique applies a peak finding technique to identify the dominating peaks in the global histograms. The peak finding algorithm could locate all the dominating peaks in the global histograms correctly and have been proven to be efficient by testing on numerous color images. As a result, the uniform regions in the image could be obtained. Since any uniform region contains 3 components representing the 3 colors of the RGB color image, each component of the uniform region is assigned one value corresponding to the intensity level of one dominating peak in their respective global histograms. Although the uniform regions are successfully obtained, some uniform regions are still perceptually close. Thus, a merging process is applied to merge these regions together.

2.1.1. Peak finding

Let us suppose dealing with color image with RGB representation which each of the primitive color components' intensity is stored in n-bit integer, giving a possible $L=2^n$ intensity levels in the interval $[0, L-1]$. Let $r(i)$, $g(i)$ and $b(i)$ be the red component, the green component and the blue component histograms, respectively. Let x_i, y_i and z_i be the number of pixels associated with ith intensity level in $r(i)$, $g(i)$ and $b(i)$, respectively.

The peak finding algorithm can be described as follows:

i. Represent the red component, green component and blue component histograms by the following equations:

$$r(i) = x_i, \tag{1}$$

$$g(i) = y_i, \tag{2}$$

$$b(i) = z_i, \tag{3}$$

where $0 \le i \le L-1$.

ii. From the original histogram, construct a new histogram curve with the following equation:

$$T_s(i) = \frac{(s(i-2)+s(i-1)+s(i)+s(i+1)+s(i+2))}{5}, \tag{4}$$

where s can be substituted by r, g and b and $2 \le i \le L-3$. $T_r(i)$, $T_g(i)$ and $T_b(i)$ are the new histogram curves constructed from the red component, green component and blue component histograms, respectively.

(Note: Based on analysis done using numerous images, the half window size can be set from 2 to 5 in this study. The half window size that is smaller than 2 could not produce a smooth histogram curve while large half window size could produce different general shape of a smooth histogram curve when comparing it to the original histogram.)

iii. Identify all peaks using the following equation:

$$P_s = ((i,T_s(i))|T_s(i) > T_s(i-1) \quad \text{and} \quad T_s(i) > T_s(i+1)), \tag{5}$$

where s can be substituted by r, g and b and $1 \le i \le L-2$. P_r, P_g and P_b are the set of peaks identified from $T_r(i)$, $T_g(i)$ and $T_b(i)$, respectively.

iv. Identify all valleys using the following equation:

$$V_s = ((i,T_s(i))|T_s(i) < T_s(i-1) \quad \text{and} \quad T_s(i) < T_s(i+1)), \tag{6}$$

where s can be substituted by r, g and b and $1 \le i \le L-2$. V_r, V_g and V_b are the set of valleys identified from $T_r(i)$, $T_g(i)$ and $T_b(i)$, respectively.

v. Remove all peaks and valleys based on the following fuzzy rule base:

IF (i is peak) *AND* ($T_s(i+1) > T_s(i-1)$)
THEN ($T_s(i) = T_s(i+1)$)
IF (i is peak) *AND* ($T_s(i+1) < T_s(i-1)$)
THEN ($T_s(i) = T_s(i-1)$)
IF (i is valley) *AND* ($T_s(i+1) > T_s(i-1)$)
THEN ($T_s(i) = T_s(i-1)$)
IF (i is valley) *AND* ($T_s(i+1) < T_s(i-1)$)
THEN ($T_s(i) = T_s(i+1)$), (7)

where s can be substituted by r, g and b and $1 \le i \le L-2$.

vi. Identify the dominating peaks in $T_r(i)$, $T_g(i)$ and $T_b(i)$ by examining the turning point which having positive to negative gradient change and the number of pixels is greater than a predefined threshold, H.

(Note: Based on analysis done using numerous images, the typical value for H is set to 20.)

2.1.2. Region initialization

After the peak finding algorithm, three sets of dominating peak's intensity level in the red, green and blue component histograms, respectively, are obtained. Let x, y and z be the number of dominating peaks identified in the red component, green component and blue component histograms, respectively. Then $P_r=(i_1, i_2, \ldots, i_x)$, $P_g=(i_1, i_2, \ldots, i_y)$ and $P_b=(i_1, i_2, \ldots, i_z)$ are the sets of dominating peak's intensity levels in the red component, green component and blue component histograms, respectively. A uniform region labeling by a cluster centroid tends to form one dominating peak in the red, green and blue component histograms, respectively. In this paper, the region initialization algorithm can be described as follows:

i. Form all the possible cluster centroids (Note: Each component of the cluster centroids can only take the intensity level of one dominating peak in the red, green and blue histogram, respectively. Thus, a number of $(x \times y \times z)$ possible cluster centroids are formed.)
ii. Assign every image pixels to the nearest cluster centroid and form the pixel set of each cluster by assigning them to their corresponding cluster centroid.
iii. Eliminate all cluster centroids that having the number of pixels assigned to them is less than a threshold, V. (Note: To reduce the initial cluster centroid number, the value for V is set to $0.006N-0.008N$ where N is the total number of pixels in that image.)
iv. Reassign every image pixels to the nearest cluster centroid. (Note: Let $\boldsymbol{c}_l$ be the lth element in the cluster centroid set and $\boldsymbol{X}_l$ be the pixel set that are assigned to $\boldsymbol{c}_l$.)
v. Update each cluster centroid, $\boldsymbol{c}_l$ by the mode of its pixel set, $\boldsymbol{X}_l$, respectively.

2.1.3. Merging

After the region initialization algorithm, the uniform regions labeling by their respective cluster centroids are obtained. Some of these regions are perceptually close and could be merged together in order to produce a more concise set of cluster centroids representing the uniform region. Thus, a merging algorithm is needed to merge these regions based on their color similarity. One of the simplest measures of color similarity is the Euclidean distance which is used to measure the color difference between two uniform regions. Let $\boldsymbol{C}=(\boldsymbol{c}_1, \boldsymbol{c}_2, \ldots, \boldsymbol{c}_M)$ be the set of cluster centroids and M be the number of cluster centroids. In this paper, the merging algorithm can be described as follows:

i. Set the maximum threshold of Euclidean distance, dc to a positive integer value.
ii. Calculate the distance, D for any two out of these M cluster centroids with the following equation:

$$D(\boldsymbol{c}_j,\boldsymbol{c}_k) = \sqrt{(R_j-R_k)^2+(G_j-G_k)^2+(B_j-B_k)^2}, \forall j \ne k, \tag{8}$$

where $1 \le j \le M$ and $1 \le k \le M$. R_j, G_j and B_j are the value of the red, green and blue component of the jth cluster centroid, respectively, and R_k, G_k and B_k are the value of the red, green and blue component of the kth cluster centroid, respectively.
iii. Find the minimum distance between two nearest cluster centroids.Merge these nearest cluster centroids to form the new cluster centroid if the minimum distance between them is less than dc. Otherwise, stop the merging process.
iv. Update the pixel set that assigned to the new cluster centroid by merging the pixel sets that assigned to these nearest cluster centroids.
v. Refresh the new cluster centroid by the mode of its pixel set.
vi. Reduce the number of cluster centroids, M to $(M-1)$ and repeat *steps ii* to *vi* until no minimum distance between two nearest cluster centroids is less than dc.(Note: Based on analysis done using numerous images, the number of cluster centroids remain constant for most of the images by varying dc from 24 to 32.)

2.2. Fuzzy C-means

The FCM algorithm is essentially a Hill-Climbing technique which was developed by Dunn in 1973 [32] and improved by Bezdek in 1981 [33]. This algorithm has been used as one of the popular clustering techniques for image segmentation in computer vision and pattern recognition. In the FCM, each image pixels having certain membership degree associated with each cluster centroids. These membership degrees having values in the range [0,1] and indicate the strength of the association between that image pixel and a particular cluster centroid.

The FCM algorithm attempts to partition every image pixels into a collection of the M fuzzy cluster centroids with respect to some given criterion [34]. Let N be the total number of pixels in that image and m be the exponential weight of membership degree. The objective function W_m of the FCM is defined as

$$W_m(\boldsymbol{U},\boldsymbol{C}) = \sum_{i=1}^{N}\sum_{j=1}^{M} u_{ji}^m d_{ji}^2, \tag{9}$$

where u_{ji} is the membership degree of ith pixel to jth cluster centroid and d_{ji} is the distance between ith pixel and jth cluster centroid. Let $\boldsymbol{U}_i=(u_{1i}, u_{2i}, \ldots, u_{Mi})^{\mathrm{T}}$ is the set of membership degree of ith pixel associated with each cluster centroids, $\boldsymbol{x}_i$ is the ith pixel in the image and $\boldsymbol{c}_j$ is the jth cluster centroid. Then $\boldsymbol{U}=(\boldsymbol{U}_1, \boldsymbol{U}_2, \ldots, \boldsymbol{U}_N)$ is the membership degree matrix and $\boldsymbol{C}=(\boldsymbol{c}_1, \boldsymbol{c}_2, \ldots, \boldsymbol{c}_M)$ is the set of cluster centroids.

The degree of compactness and uniformity of the cluster centroids greatly depend on the objective function of the FCM. In general, a smaller objective function of the FCM indicates a more compact and uniform cluster centroid set. However, there is no close form solution to produce minimization of the objective function.

To achieve the optimization of the objective function, an iteration process must be carried out by the FCM algorithm. In this paper, the FCM is employed to improve the compactness of the clusters produced by the histogram thresholding module. The FCM can be described as follows:

i. Set the iteration terminating threshold, ε to a small positive number in the range [0,1] and the number of iteration q to 0.
ii. Calculate $\boldsymbol{U}^{(q)}$ according to $\boldsymbol{C}^{(q)}$ with the following equation:

$$u_{ji} = \frac{1}{\sum_{k=1}^{M} (d_{ji}/d_{ki})^{2/(m-1)}}, \tag{10}$$

where $1 \le j \le M$ and $1 \le i \le N$. Notice that if $d_{ji}=0$, then $u_{ji}=1$ and set others membership degrees of this pixel to 0.
iii. Calculate $\boldsymbol{C}^{(q+1)}$ according to $\boldsymbol{U}^{(q)}$ with the following equation:

$$c_j = \frac{\sum_{i=1}^{N} u_{ji}^m \boldsymbol{x}_i}{\sum_{i=1}^{N} u_{ji}^m}, \tag{11}$$

where $1 \le j \le M$.
iv. Update $\boldsymbol{U}^{(q+1)}$ according to $\boldsymbol{C}^{(q+1)}$ with Eq. (10).
v. Compare $\boldsymbol{U}^{(q+1)}$ with $\boldsymbol{U}^{(q)}$. If $\|\boldsymbol{U}^{(q+1)} - \boldsymbol{U}^{(q)}\| \le \varepsilon$, stop iteration. Otherwise, $q=q+1$, and repeat *steps ii* to *iv* until $\|\boldsymbol{U}^{(q+1)} - \boldsymbol{U}^{(q)}\| > \varepsilon$.

3. Illustration of the implementation procedure

In this section, we apply the HTFCM approach to perform the segmentation with the 256×256 image *House* depicted in Fig. 1(a). Figs. 2(a), 3(a) and 4(a) show the red, green and blue component histogram of the image, respectively. In Fig. 2(a), the dominating peaks that could represent the red component of dominant regions are difficult to be recognized as a large number of small peaks exist in the histogram. The similar case has also been shown in Figs. 3(a) and 4(a). These small peaks must be removed so that the dominating peaks can be recognized effectively. Thus, the dominating peaks are recognized according to the proposed peak finding technique. Figs. 2(b), 3(b) and 4(b) show the resultant histogram curves, after applying the proposed peak finding technique. Since the general shape of each resultant histogram curve have a great similarity with their respective original histogram, the dominating peak in the histogram curve can be considered as the dominating peak in their respective histogram. Furthermore, each of the resultant histogram curves gives better degree of smoothness than their respective original histogram. As a result, the dominating peaks in the histogram can be recognized easily by examining the histogram curve. Then, the initial clusters are formed by assigning every pixel to their cluster centroids, respectively. For example, the left uppermost pixel in the image having the RGB value of (159, 197, 222) is assigned to the centroid having the RGB value of (159, 199, 224) since the Euclidean distance between the pixel and the centroid is the shortest compared to other centroids. The RGB value of

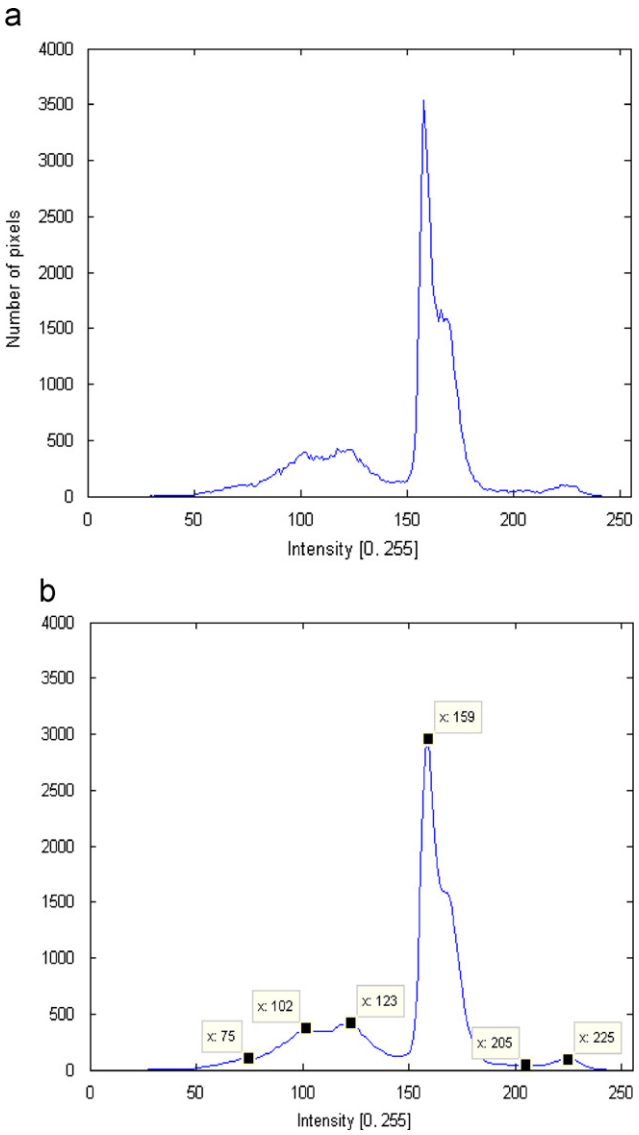

Fig. 2. (a) Red component histogram of image *House*, (b) resultant histogram curve after peak finding technique (Note: The intensity level of the dominating peaks is labeled by x).

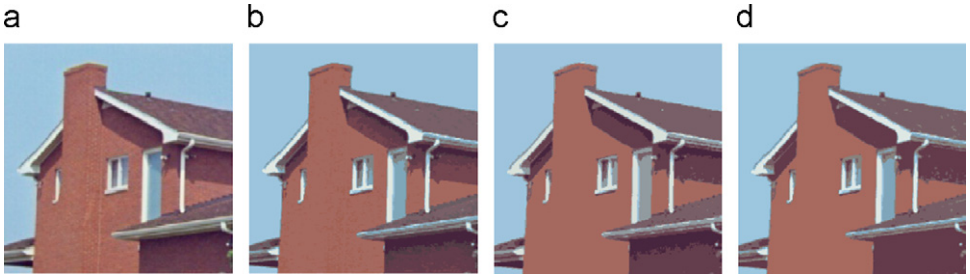

Fig. 1. Image *House* and its segmentation results. (a) Original image *House*, (b) image after cluster centroid initialization, (c) image after merging and (d) final segmentation result.

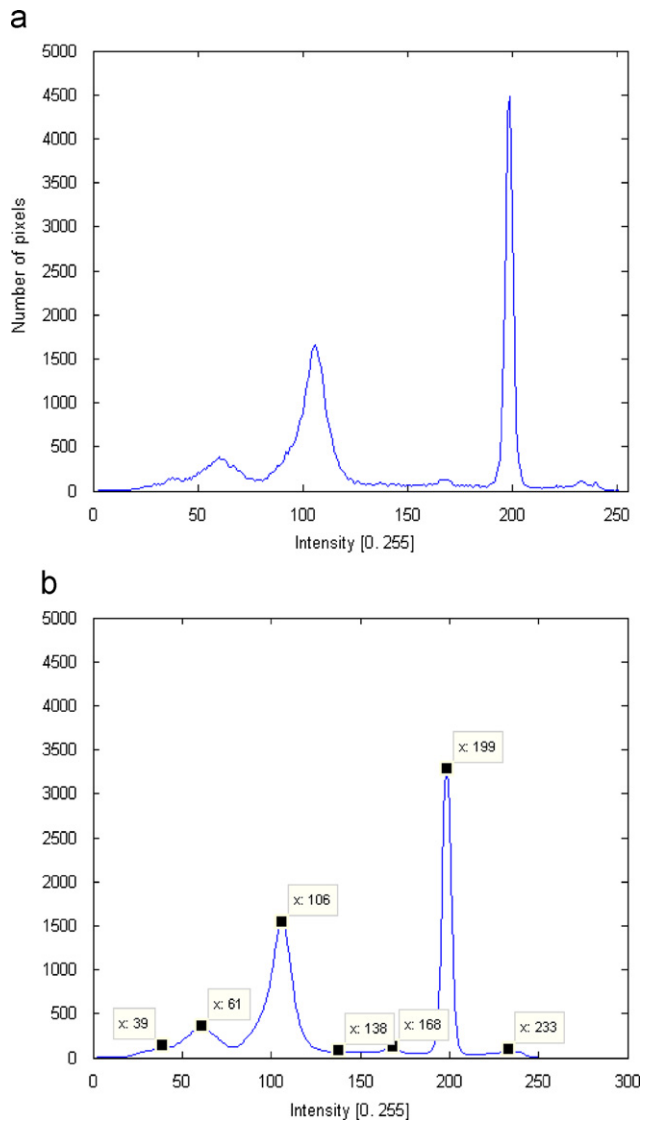

Fig. 3. (a) Green component histogram of image *House* and (b) resultant histogram curve after peak finding technique (Note: The intensity level of the dominating peaks is labeled by *x*.).

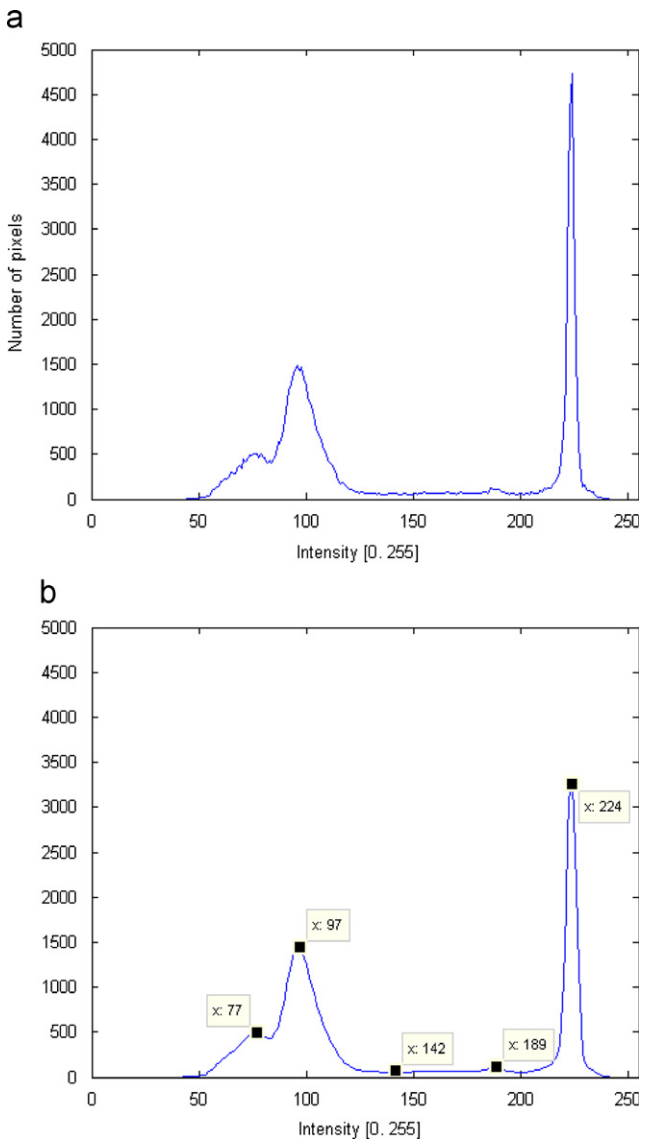

Fig. 4. (a) Blue component histogram of image *House* and (b) resultant histogram curve after peak finding technique (Note: The intensity level of the dominating peaks is labeled by *x*.).

the centroid is obtained from one of the dominating peaks in Figs. 2(b), 3(b) and 4 (b), respectively. The result of initial clusters is illustrated in Fig. 1(b). Next, the merging process is carried out to merge all the clusters that are perceptually close. This merging process is able to reduce the cluster number and keep a reasonable cluster number for all kinds of input images. The result of the merging process is illustrated in Fig. 1(c). Finally, the FCM algorithm is applied to perform color segmentation. The final segmentation result is illustrated in Fig. 1(d).

4. Experiment results

The HTFCM approach has been tested on more than 200 images taken from public image segmentation databases. In this paper, 30 images are selected to demonstrate the capability of the proposed HTFCM approach. 8 out of these images namely *House* (256×256), *Football* (256×256), *Golden Gate* (256×256), *Smarties* (256×256), *Capsicum* (256×256), *Gantry Crane* (400×264), *Beach* (321×481) and *Girl* (321×481) are evaluated in details to highlight the advantages of the proposed HTFCM approach. While another 22 images are presented as supplementary images to further support the findings. The AS, the AFHA and the IAFHA approaches which are proved to be able to provide good solution to overcome the FCM's sensitiveness to the initialization conditions of cluster centroids and centroid number are used as comparison in order to see whether the HTFCM approach could result in generally better performance and cluster quality than these approaches. The performance of the HTFCM approach is evaluated by comparing the algorithmic efficiency and the segmentation results with the AS, the AFHA and the IAFHA approaches. In this study, we fix *dc* as 28 since it tend to produce reasonable results for the AS, the AFHA, the IAFHA [26] and the HTFCM approaches.

4.1. Evaluation on segmentation results

In this section, the segmentation results for the AS, the AFHA, the IAFHA and the HTFCM approaches are evaluated visually. Generally, as shown in Figs. 5–12, the proposed HTFCM approach produces better segmentation results as compared to the AS, the

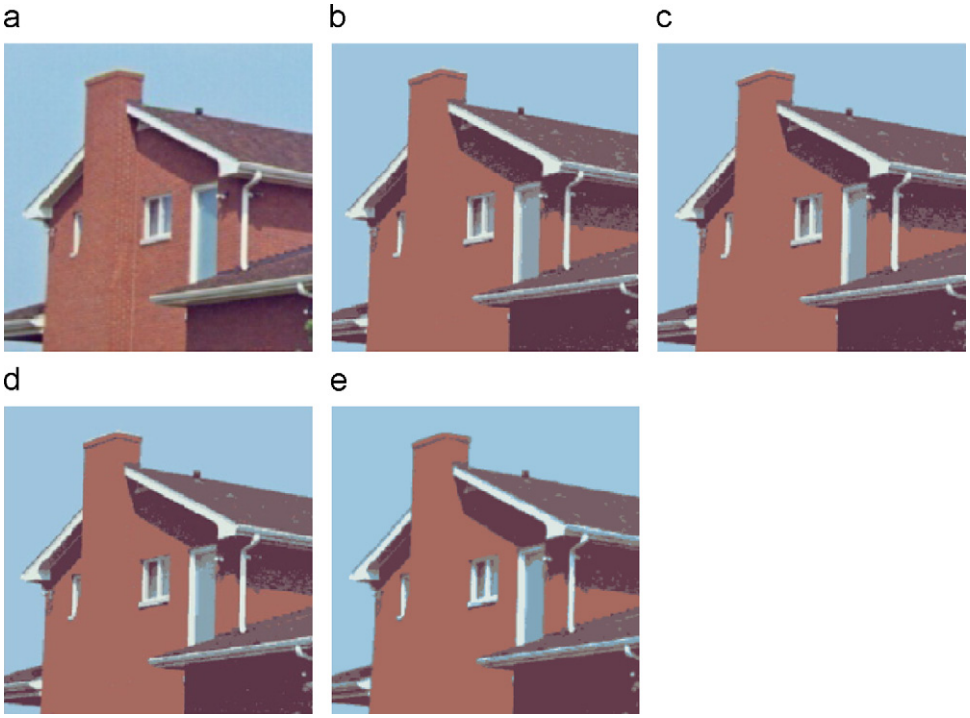

Fig. 5. The image *House*: (a) original image, and the rest are segmentation results of the test image by various algorithms (b) AS, (c) AFHA, (d) IAFHA, and (e) HTFCM.

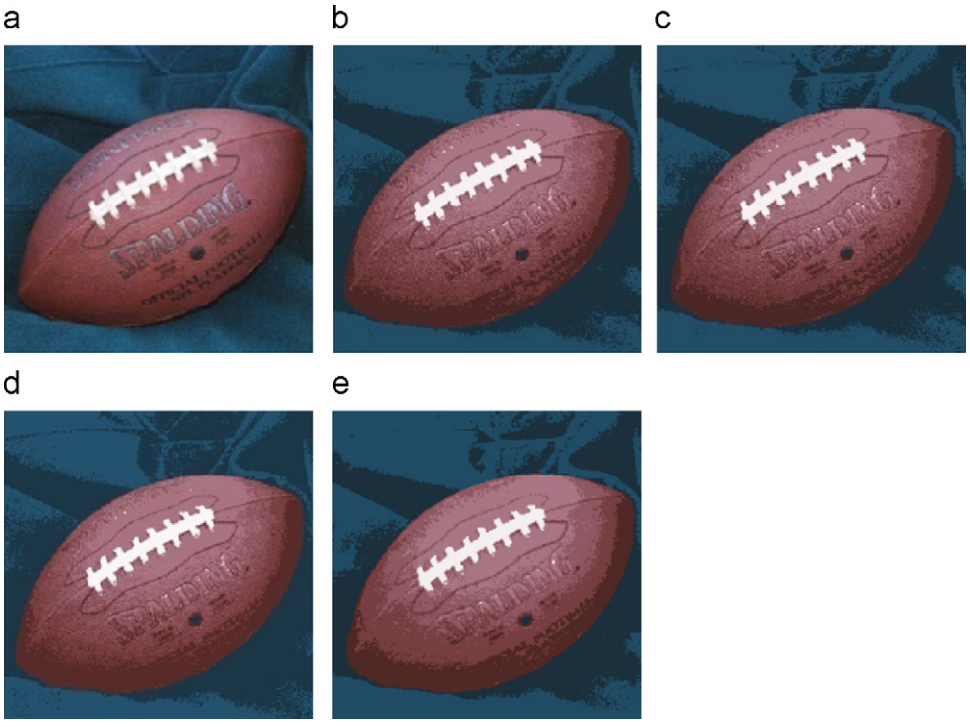

Fig. 6. The image *Football*: (a) original image, and the rest are segmentation results of the test image by various algorithms (b) AS, (c) AFHA, (d) IAFHA, and (e) HTFCM.

AFHA and the IAFHA approaches. The segmented regions of the resultant images produced by the HTFCM approach are more homogeneous. For example, notice for the image *House*, the HTFCM approach gives better segmentation result than the AS, the AFHA and the IAFHA approaches by producing more homogeneous house roof and walls as depicted in Fig. 5. In the image *Football*, the HTFCM approach also outperforms the AS, the AFHA and the IAFHA approaches by giving more homogeneous background as shown in Fig. 6. As for the image *Golden Gate*, although the AS, the AFHA and the IAFHA approaches produce homogeneous sky region, but an obvious classification error could be seen where these approaches mistakenly assign considerable pixels of the leave of tree as part of the bridge. The proposed HTFCM approach successfully avoids this classification error and furthermore, produces more homogeneous hill and sea regions as shown in Fig. 7. In the image *Capsicum*, the proposed HTFCM

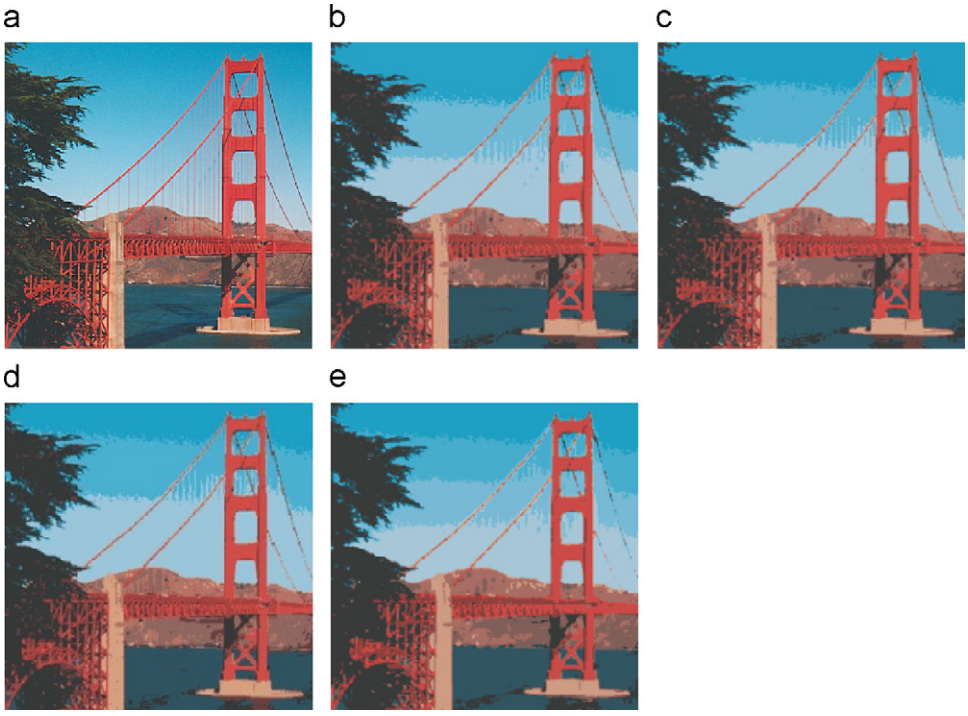

Fig. 7. The image *Golden Gate*: (a) original image, and the rest are segmentation results of the test image by various algorithms (b) AS, (c) AFHA, (d) IAFHA, and (e) HTFCM.

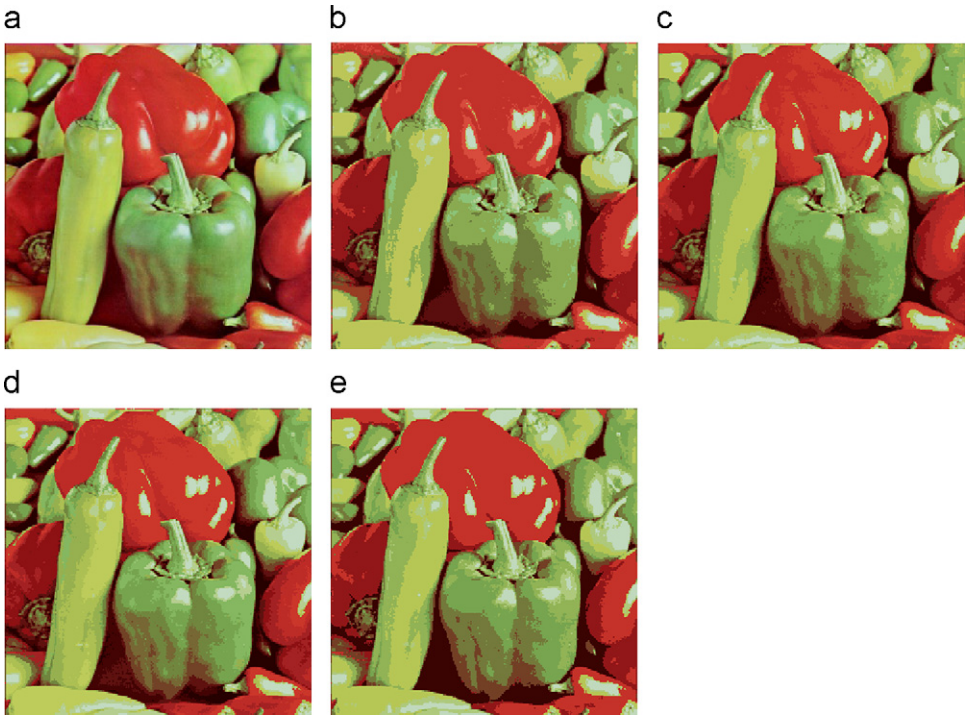

Fig. 8. The image *Capsicum*: (a) original image, and the rest are segmentation results of the test image by various algorithms (b) AS, (c) AFHA, (d) IAFHA, and (e) HTFCM.

approach also outperforms other techniques by producing more homogeneous red capsicum as depicted in Fig. 8. Notice for the image *Smarties*, the AS, the AFHA and the IAFHA approaches mistakenly assign considerable pixels of the background as part of the green Smarties. The proposed HTFCM approach successfully avoids this classification error and furthermore, produces more homogeneous background as shown in Fig. 9. As for the image *Beach*, the HTFCM approach outperforms others approaches by giving more homogeneous beach and sea as depicted in Fig. 10. As for the image *Gantry Crane*, there is a classification error where part of the left-inclined truss has been assigned to the sky by the AS, the AFHA and the IAFHA approaches as shown in Fig. 11. The proposed HTFCM successfully avoids this classification error. The similar result is obtained for the image *Girl*. The HTFCM approach outperforms other approaches by classifying the blue and red part of the shirt as single cluster while the AS,

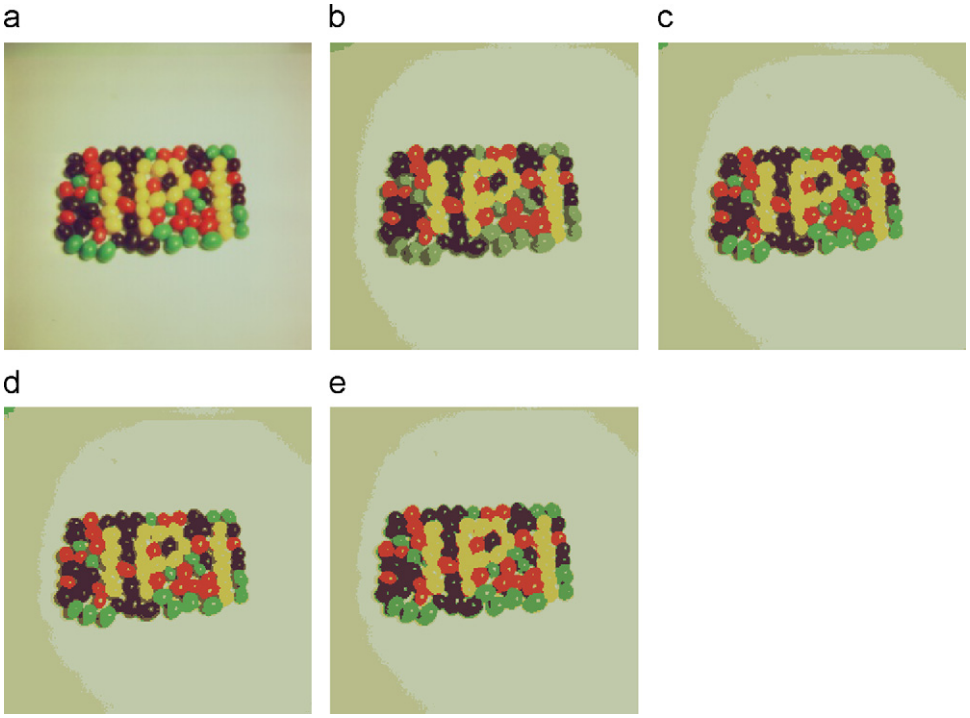

Fig. 9. The image *Smarties*: (a) original image, and the rest are segmentation results of the test image by various algorithms (b) AS, (c) AFHA, (d) IAFHA, and (e) HTFCM.

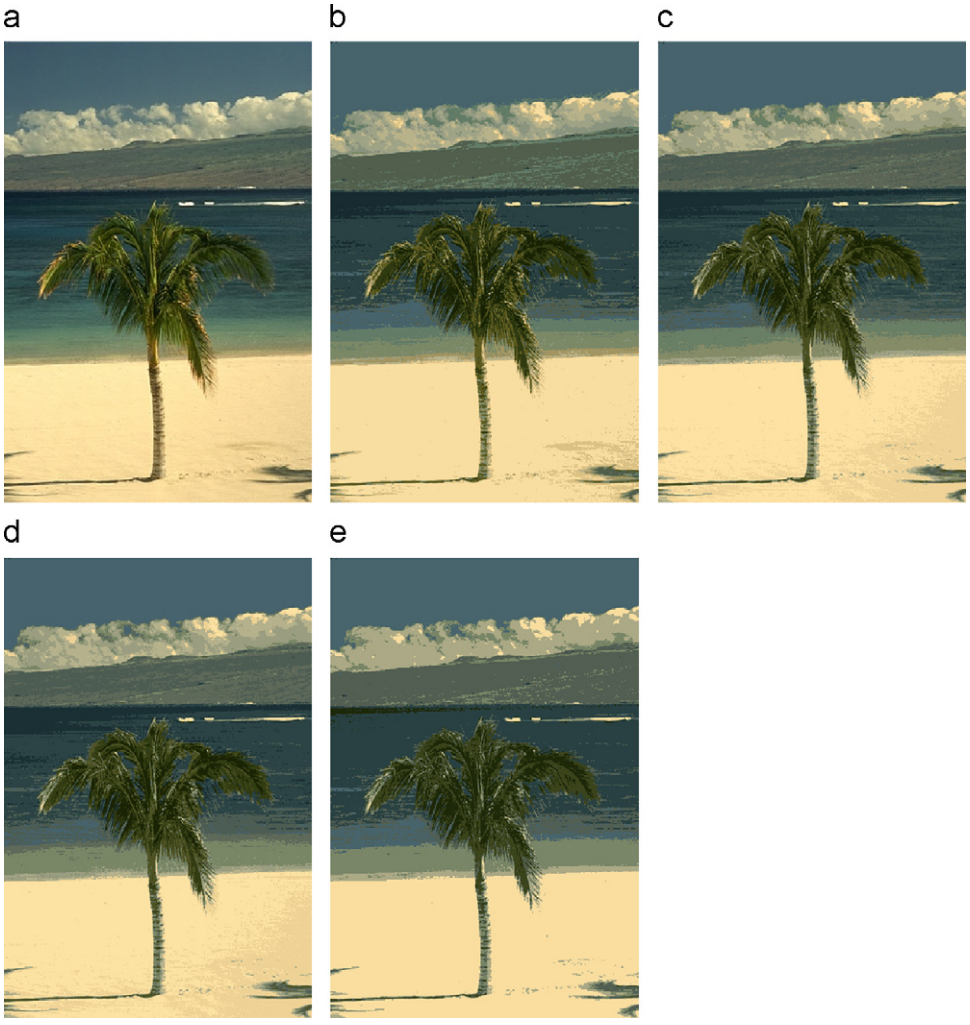

Fig. 10. The image *Beach*: (a) original image, and the rest are segmentation results of the test image by various algorithms (b) AS, (c) AFHA, (d) IAFHA, and (e) HTFCM.

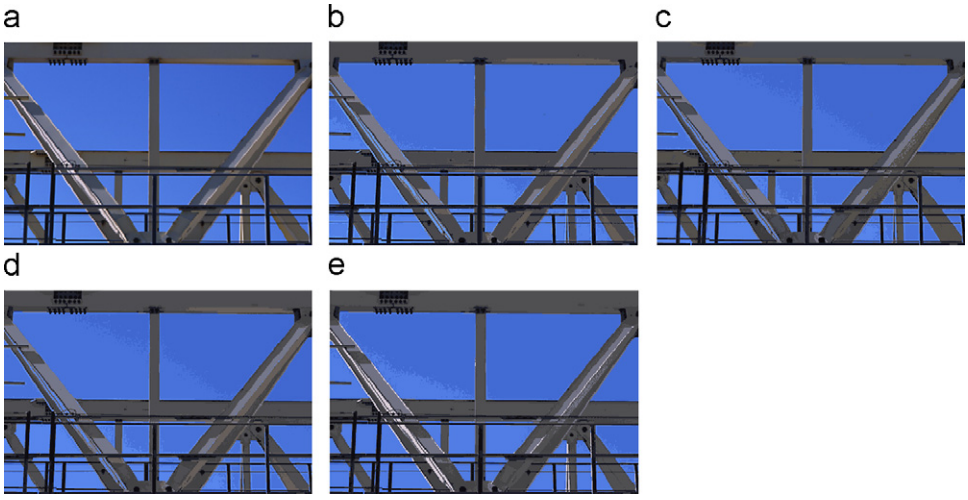

Fig. 11. The image *Gantry Crane*: (a) original image, and the rest are segmentation results of the test image by various algorithms (b) AS, (c) AFHA, (d) IAFHA, and (e) HTFCM.

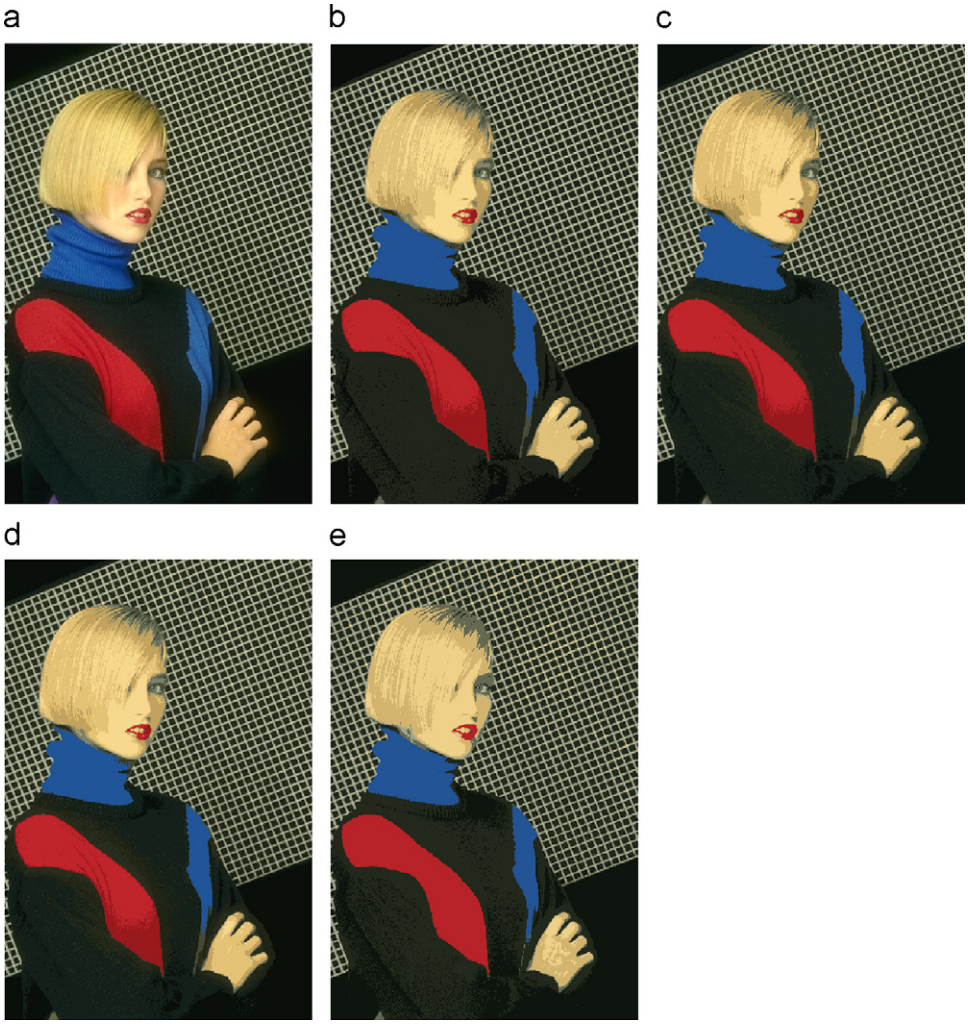

Fig. 12. The image *Girl*: (a) original image, and the rest are segmentation results of the test image by various algorithms (b) AS, (c) AFHA, (d) IAFHA, and (e) HTFCM.

the AFHA and the IAFHA approaches can only classify the blue part of the shirt as single cluster.

The aforementioned findings are also supported by the results obtained from the 22 supplementary images as shown in Fig. 13 in Appendix A. The results clearly prove that the proposed HTFCM approach outperforms the AS, the AFHA and the IAFHA approaches by significantly producing more homogeneous regions.

Another main advantage of the proposed HTFCM approach, based on the segmentation results, the HTFCM approach outperforms the AS, the AFHA and the IAFHA approaches by automatically assigning fewer clusters with fewer regions especially when segmenting relatively simple natural images such as *House*, *Football*, *Smarties* and *Gantry Crane*. Due to the reason that the AS, the AFHA and the IAFHA approaches posses the same decision mechanism, these approaches always give almost similar cluster number. The number of regions produced by each approach is provided in Table 1.

4.2. Evaluation on cluster quality

To evaluate the cluster quality, several important cluster validity criterions have been featured by previous works on fuzzy clustering. In this paper, we adopt two evaluation functions to serves as the quantitative benchmarks that could be used to evaluate the cluster quality. The first benchmark is Bezdek's partition coefficient [35], where the evaluation function is defined as follows:

$$V_{PC} = \frac{\sum_{i=1}^{N}\sum_{j=1}^{M} u_{ji}^2}{N}. \tag{12}$$

The properties of this cluster validity evaluation model were studied in [35,36]. This benchmark is used to measure the fuzziness of a clustering result and the V_{PC} value can take on any value ranges from 0 to 1. From the context of validation, a good clustering algorithm must produce a better clustering result that is less fuzzy with larger V_{PC} value.

The second benchmark is the Xie–Beni function [37], where the evaluation function is defined as follows:

$$V_{XB} = \frac{\sum_{i=1}^{N}\sum_{j=1}^{M} u_{ji}^2 x_i - c_j^2}{N \min_{\forall j \neq k}\{c_j - c_k^2\}}. \tag{13}$$

According to Xie and Beni, the V_{XB} should decrease monotonically when the cluster number is close to the number of pixels in the image and furthermore, a better clustering result should produce smaller V_{XB} value. This accords with our segmentation applications since we would like regions is visually as different as possible.

4.2.1. V_{PC} test

The V_{PC} values of the AS, the AFHA, the IAFHA and the HTFCM approaches are tabulated in Table 2. It is interesting to see that the HTFCM approach always produces relatively larger V_{PC} values

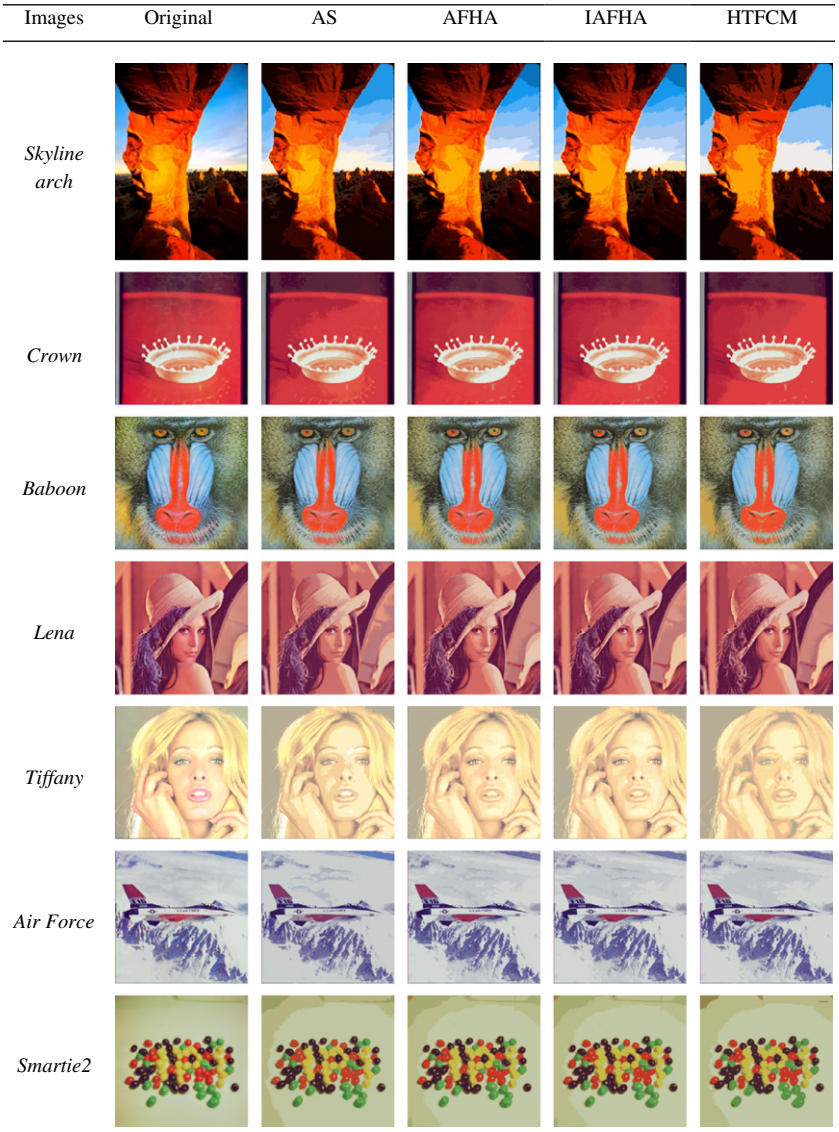

Fig. 13. The images and segmentation results of the test images by the AS, the AFHA, the IAFHA, and the HTFCM algorithms.

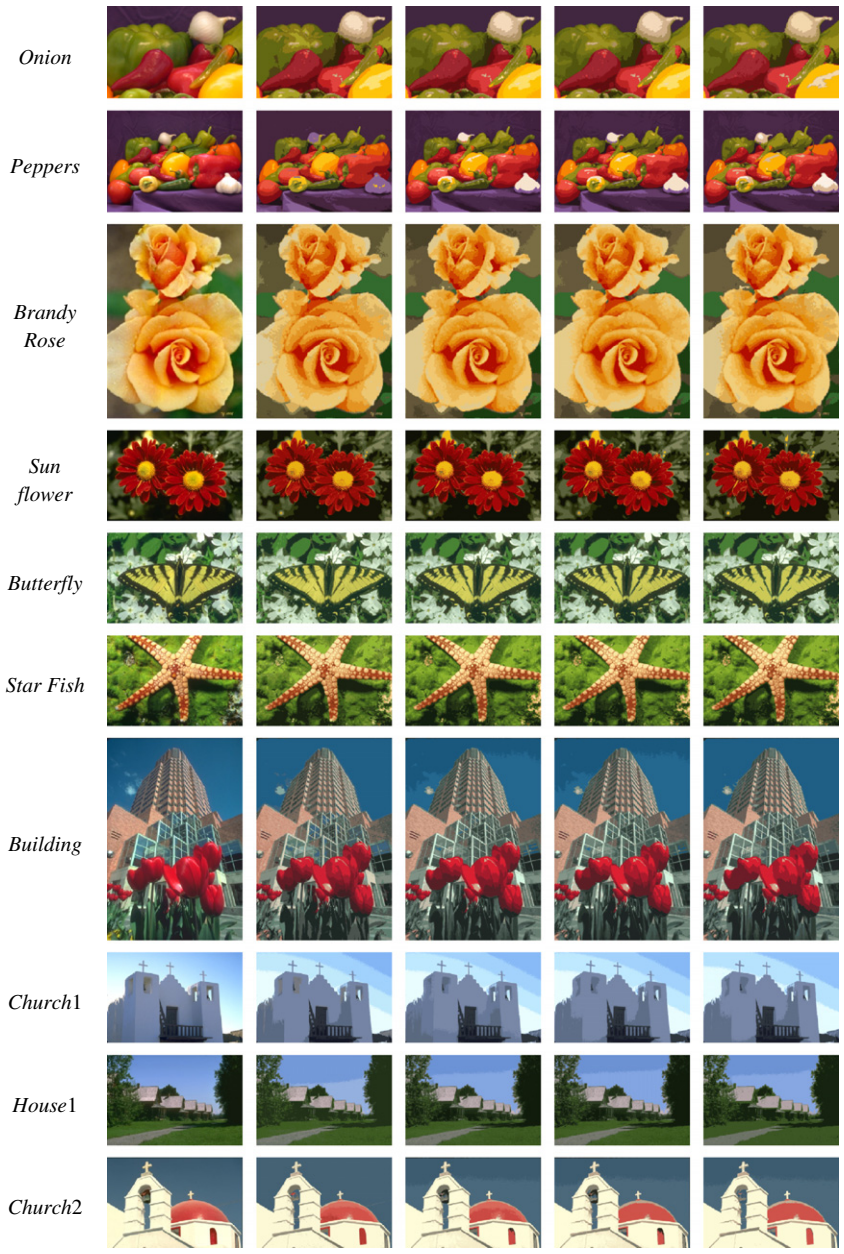

Fig. 13. (*Continued*)

than other approaches, showing that the general cluster distribution is better than other approaches. Thus, the HTFCM approach outperforms the AS, the AFHA and the IAFHA approaches by giving better cluster quality.

Apart from these images, the V_{PC} values of the AS, the AFHA, the IAFHA and the HTFCM approaches for another 22 supplementary images are tabulated in Table 7 in Appendix B. In general, the proposed HTFCM algorithm outperforms the AS, the AFHA and the IAFHA algorithms by giving relatively larger average V_{PC} value of these 22 images.

4.2.2. V_{XB} test

The V_{XB} values of the AS, the AFHA, the IAFHA and the HTFCM approaches are tabulated in Table 3. Notice for the image *Girl*, it is interesting to see the AS produces relatively smaller V_{XB} value than other approaches while for the image *Beach*, the IAFHA outperforms others. In the images *Football*, *Golden Gate*, *Capsicum*, *Smarties* and *Gantry Crane*, the HTFCM approach outperforms the AS, the AFHA and the IAFHA approaches by giving smaller V_{XB} value. In the image *House*, the IAFHA and the HTFCM approaches have comparable V_{XB} value as indicated in Table 3 and both the IAFHA and the HTFCM approaches outperform the AS and the AFHA approaches by producing smaller V_{XB} value.

Furthermore, the results of V_{XB} test for the 22 images shown in Fig. 13 in Appendix A also prove that the proposed HTFCM approach outperforms other approaches by giving smaller average V_{XB} value as tabulated in Table 7 in Appendix B.

4.3. Comparison of algorithm efficiency

In this section, the efficiency of the HTFCM approach and other approaches are compared as the execution time imposes a large influence upon the practicability of the approach especially in consumer electronic products. The execution times

Fig. 13. (*Continued*)

Table 1
Number of regions produced by different algorithms.

Images	Algorithms			
	AS	AFHA	IAFHA	**HTFCM**
House	10	10	10	**7**
Football	10	10	10	**7**
Golden Gate	16	16	16	**11**
Capsicum	15	15	17	**8**
Smarties	7	7	7	**6**
Beach	15	15	14	**10**
Gantry Crane	10	10	9	**8**
Girl	14	14	15	**9**

The bold values represent the best results obtained for the comparison.

Table 2
Comparison of results for different algorithms in V_{PC} test.

Images	Algorithms			
	AS	AFHA	IAFHA	**HTFCM**
House	0.742	0.736	0.729	**0.804**
Football	0.628	0.633	0.634	**0.679**
Golden Gate	0.548	0.549	0.550	**0.604**
Capsicum	0.474	0.464	0.449	**0.593**
Smarties	0.771	0.784	0.782	**0.793**
Beach	0.593	0.587	0.603	**0.689**
Gantry Crane	0.648	0.631	0.649	**0.691**
Girl	0.654	0.629	0.596	**0.668**

The bold values represent the best results obtained for the comparison.

Table 3
Comparison of results for different algorithms in V_{XB} test.

Images	Algorithms			
	AS	AFHA	IAFHA	**HTFCM**
House	0.120	0.118	**0.086**	0.088
Football	0.171	0.115	0.122	**0.094**
Golden Gate	0.131	0.184	0.220	**0.122**
Capsicum	0.161	0.558	0.439	**0.221**
Smarties	0.107	0.111	0.120	**0.106**
Beach	0.237	0.231	**0.189**	0.253
Gantry Crane	0.405	0.726	0.607	**0.383**
Girl	**0.114**	0.385	0.526	0.299

The bold values represent the best results obtained for the comparison.

Table 4
Execution time (in seconds) of different algorithms.

Images	Algorithms			
	AS	AFHA	IAFHA	**HTFCM**
House	22.0	24.1	14.6	**10.6**
Football	29.7	35.2	15.3	**8.2**
Golden Gate	53.3	59.9	37.1	**15.6**
Capsicum	28.8	35.3	20.5	**13.8**
Smarties	11.6	14.7	8.2	**7.4**
Beach	20.8	23.6	17.2	**14.9**
Gantry Crane	16.6	20.4	19.7	**14.7**
Girl	61.2	87.0	45.6	**24.3**

The bold values represent the best results obtained for the comparison.

for these segmentation approaches are tabulated in Table 4. The execution times of the AS, the AFHA and the IAFHA are relatively longer than the HTFCM when segmenting all of these eight images. The reason lies in the fact that the AS, the AFHA and the IAFHA approaches are suffering from high computational complexity. Therefore, the HTFCM approach has greater efficiency due to its simplicity.

4.4. Further comparison analysis with the IAFHA

Although the AS, the AFHA and the IAFHA approaches produce comparable cluster quality, the IAFHA approach has better algorithmic efficiency than the AS and the AFHA approaches by incorporating an ant sub-sampling based method to reduce the computational complexity of the AS and the AFHA approaches.

Thus, only the IAFHA approach is compared with the HTFCM approach.

In this section, three benchmarks are applied for quantitative evaluation of the segmentation results. These benchmarks are used to estimate the segmentation results with some human characterization about the properties of ideal segmentation and require no prior knowledge of correct segmentation. These three functions are, respectively:

$F(I)$ proposed by Liu and Yang [38]

$$F(I)=\frac{\sqrt{M}\sum_{j=1}^{M} e_j^2}{\sqrt{N_j}}, \tag{14}$$

$F'(I)$ proposed by Borsotti et al. [39]

$$F'(I)=\frac{\frac{1}{(1000\times N)}\sqrt{\sum_{a=1}^{MaxArea}[S(a)]^{1+(1/a)}}\sum_{j=1}^{M} e_j^2}{\sqrt{N_j}}, \tag{15}$$

$Q(I)$ further refined from $F(I)$ by Borsotti et al. [39] as

$$Q(I)=\frac{1}{(1000\times N)}\sqrt{M}\sum_{j=1}^{M}\left[\frac{e_j^2}{1+\log N_j}+\left(\frac{S(N_j)}{N_j}\right)^2\right]. \tag{16}$$

For the above three formulae, I is an image and N is the total pixels in I. The segmentation can be described as an assignment of pixels in the image I into M regions. Let C_j denotes the set of pixels in region j, $N_j=|C_j|$ denotes the number of pixels in C_j, e_j is defined as the Euclidean distances between the RGB color vectors of the pixels of region j and the color vector attributed to region j in the segmented image. Finally, $S(a)$ denotes the number of regions in image I that has an area of exactly a and $MaxArea$ denotes the largest region in the segmented image. Although the above three formulae are different, these functions are used to penalize segmentation that form too many regions and having non-homogeneous regions by giving a larger values.

The quantitative evaluation on segmentation results are tabulated in Table 5 for images shown in Figs. 5–12. The quantitative evaluation on segmentation results for the supplementary images shown in Fig. 13 in Appendix A are tabulated in Table 8 in Appendix C. Note that all of the evaluation functions have favored segmentation by the HTFCM approach by giving relatively small values for these three evaluation benchmarks. The results obtained also show that the

Table 5
Quantitative evaluation on segmentation of selected images.

Algorithm	Images	$F(I)$ (*1.0e+8)	$F'(I)$	Q(I) (*1.0e+3)
HTFCM	*House*	**0.0495**	7.4898	**0.1237**
	Football	**0.0653**	**9.9564**	**0.1895**
	Golden Gate	**0.1312**	**20.0224**	**0.3142**
	Capsicum	**0.1404**	**21.4299**	**0.3606**
	Smarties	**0.0614**	9.3691	**0.1442**
	Beach	**0.1169**	**7.5733**	**0.1495**
	Gantry Crane	**0.0960**	**9.1191**	**0.1717**
	Girl	**0.1593**	**10.3179**	**0.1864**
IAFHA	*House*	0.2168	**6.3619**	0.4004
	Football	0.3367	17.8547	0.8403
	Golden Gate	0.6647	28.2005	0.4904
	Capsicum	0.1711	26.1030	0.3806
	Smarties	0.0625	**9.2325**	0.1456
	Beach	0.1179	7.6361	0.1513
	Gantry Crane	0.1793	16.9766	0.3166
	Girl	0.1886	12.2131	0.2987

The bold values represent the best results obtained for the comparison.

Table 6
Mean values for quantitative evaluation on segmentation of these 8 images.

Algorithm	F(I) (*1.0e+8)	F'(I)	Q(I) (*1.0e+3)
HTFCM	**0.1025**	**11.9097**	**0.2050**
IAFHA	0.2422	15.5723	0.3780

The bold values represent the best results obtained for the comparison.

Table 7
Comparison of results for different algorithms in V_{PC} and V_{XB} tests.

Images	V_{PC}				V_{XB}			
	AS	AFHA	IAFHA	HTFCM	AS	AFHA	IAFHA	HTFCM
Skyline Arch	0.541	0.579	0.585	**0.685**	0.255	0.342	0.302	**0.254**
Crown	0.539	0.524	0.524	**0.613**	0.536	0.453	0.453	**0.260**
baboon	0.281	0.297	0.284	**0.343**	0.391	**0.303**	0.339	0.328
Lena	0.422	0.468	0.453	**0.482**	0.315	0.316	**0.284**	0.289
Tiffany	0.518	0.519	0.520	**0.646**	0.249	0.252	0.250	**0.237**
Air Force	0.652	0.651	0.670	**0.690**	0.224	0.191	0.188	**0.181**
Smarties2	0.705	0.711	0.711	**0.750**	0.150	0.148	0.148	**0.140**
Onions	0.496	0.489	0.500	**0.531**	0.339	0.395	0.370	**0.309**
Peppers	0.476	0.498	0.513	**0.525**	0.767	**0.718**	0.820	0.720
Brandy Rose	0.468	**0.488**	0.468	0.464	0.286	0.250	**0.228**	0.249
Sun flower	0.616	0.631	0.621	**0.671**	0.234	0.258	0.177	**0.134**
Butterfly	0.473	0.478	0.480	**0.584**	0.460	0.437	0.350	**0.255**
Star Fish	0.489	0.497	0.505	**0.546**	0.273	0.276	0.279	**0.170**
Building	0.452	**0.498**	0.472	0.486	0.251	**0.248**	0.269	0.288
Church1	0.694	0.713	0.746	**0.761**	0.135	0.136	0.117	**0.107**
House1	0.601	0.636	0.637	**0.758**	0.269	0.267	**0.219**	0.228
Church2	0.780	0.753	0.771	**0.814**	0.256	**0.216**	0.283	0.254
Sky	0.565	0.583	0.583	**0.680**	0.349	0.294	0.294	**0.149**
House3	0.656	0.668	0.670	**0.749**	0.218	0.182	**0.140**	0.143
Church3	0.595	0.586	0.586	**0.646**	0.270	0.214	0.272	**0.140**
Car1	0.416	0.450	0.453	**0.488**	0.287	0.234	**0.217**	0.250
Car2	0.549	0.549	0.550	**0.604**	0.566	0.536	0.541	**0.347**
Average	0.545	0.558	0.559	**0.614**	0.322	0.303	0.297	**0.247**

The bold values represent the best results obtained for the comparison.

Table 8
Quantitative evaluation on segmentation of selected images.

Images	IAFHA			HTFCM		
	$F(I)$ (*1.0e+8)	$F'(I)$	$Q(I)$ (*1.0e+3)	$F(I)$ (*1.0e+8)	$F'(I)$	$Q(I)$ (*1.0e+3)
Skyline Arch	0.3529	19.9789	**0.4377**	**0.3483**	**19.7186**	0.4445
Crown	0.2004	7.6451	0.1973	**0.1792**	**6.8347**	**0.1884**
baboon	0.6452	24.6112	0.5908	**0.5967**	**22.7634**	**0.5597**
Lena	**0.1979**	**7.5505**	0.2961	0.1995	7.6116	**0.2120**
Tiffany	0.2123	8.0978	0.1990	**0.1338**	**5.1050**	**0.1906**
Air Force	0.1718	6.5554	0.1445	**0.1472**	**5.6149**	**0.1379**
Smarties2	**0.1416**	**5.4029**	0.1972	0.1559	5.9453	**0.1632**
Onions	**0.3752**	**20.9947**	**0.3895**	0.3761	21.0462	0.4307
Peppers	0.4931	25.0809	0.4684	**0.4295**	**21.8462**	**0.4190**
Rose	0.2561	14.0092	0.3188	**0.2550**	**13.9481**	**0.3147**
Sun flower	0.2989	17.0707	0.3234	**0.2838**	**16.2085**	**0.3070**
Butterfly	0.1698	9.6995	0.3888	**0.1612**	**9.2085**	**0.3871**
Star Fish	0.2583	14.7508	0.3080	**0.2427**	**13.8600**	**0.3079**
Building	0.2934	16.7533	**0.3019**	**0.2932**	**16.7443**	0.3324
Church1	**0.0793**	**4.5295**	0.1292	0.0828	4.7286	**0.1207**
House1	**0.1096**	**6.2573**	0.1977	0.1115	6.3683	**0.1888**
Church2	0.1351	7.7137	0.2511	**0.1279**	**7.3027**	**0.1906**
Sky	**0.1102**	**6.2948**	0.2387	0.1105	6.3132	**0.1943**
House3	**0.0949**	**5.4196**	0.2191	0.1104	6.3043	**0.1822**
Church3	0.1653	9.4398	**0.1834**	**0.1588**	**9.0673**	0.2162
Car1	0.3826	14.5948	0.3372	**0.3488**	**13.3062**	**0.3298**
Car2	0.7329	17.0077	0.2300	**0.3994**	**15.1723**	**0.1501**
Average	0.2671	12.2481	0.2885	**0.2387**	**11.5917**	**0.2713**

The bold values represent the best results obtained for the comparison.

HTFCM approach tends to favor results with smaller cluster numbers.

The mean values for quantitative evaluation on segmentation of the IAFHA and the HTFCM approaches on these 8 images are tabulate in Table 6. It is clearly seen that the proposed HTFCM outperforms the IAFHA approach.

Although the proposed HTFCM could produce good segmentation results, it still can be improved. As indicated in Figs. 3(b), 4(b) and 5(b), it can be obviously seen that some small peaks that reside in nearly flat portion of the histogram curves had been recognized as dominating peaks. To get rid of these dominating peaks, the peak's sharpness or area could be examined for feasible future work.

5. Conclusions

This paper presented the histogram thresholding – fuzzy C-means (HTFCM) hybrid approach that could find different application in pattern recognition as well as in computer vision, particularly in color image segmentation. Our approach could provide a good solution to overcome the FCM's sensitiveness to the initialization condition of cluster centroids and centroid number by using the histogram thresholding technique. Due to the simplicity of implementation, our approach could give better algorithm efficiency over the AS, the AFHA and the IAFHA segmentation approaches, which suffer from high computational complexity in their implementations. Furthermore, our approach could also obtain better segmentation results over these approaches by producing a fewer number of regions as well as providing more homogeneous segmented regions.

Acknowledgements

The authors would like to express their sincere thanks to the associate editor and all reviewers who made great contributions to the improvement of the final paper. This research was supported by Universiti Sains Malaysia under Research University (RU) Grant entitled 'Imaging' and Postgraduate Fellowship Scheme.

Appendix A. Segmentation results of the test images by the AS, the AFHA, the IAFHA and the HTFCM algorithms

See Fig. 13.

Appendix B. Comparison of results for the AS, the AFHA, the IAFHA and the HTFCM algorithms in V_{PC} and V_{XB} tests

See Table 7.

Appendix C. Quantitative evaluation on segmentation of the test images by the IAFHA and the HTFCM algorithms

See Table 8.

References

[1] Y. Rui, T.S. Huang, S.-F. Chang, Image retrieval: current techniques, promising directions, and open issues, J. Vis. Commun. Image Represent. 10 (1) (1999) 39–62.
[2] A.W.M. Smeulders, M. Worring, S. Santini, A. Gupta, R. Jain, Content-based image retrieval at the end of the early years, IEEE Trans. Pattern Anal. Mach. Intell. 22 (12) (2000) 1349–1380.
[3] B.S. Manjunath, J.-R. Ohm, V.V. Vasudevan, A. Yamada, Color and texture descriptors, IEEE Trans. Circuits Syst. Video Technol. 11 (6) (2001) 703–715.
[4] A. Mojsilovic, J. Kovacevic, J. Hu, R.J. Safranek, K. Ganapathy, Matching and retrieval based on the vocabulary and grammar of color patterns, IEEE Trans. Image Process. 9 (1) (2000) 38–54.
[5] G. Derefeldt, T. Swartling, Color concept retrieval by free color naming – identification of up to 30 colors without training, Displays 16 (1995) 69–77.
[6] K.S. Deshmukh, G.N. Shinde, An adaptive color image segmentation, Electron. Lett. Comput. Vis. Image Anal. 5 (4) (2005) 12–23.
[7] C. Carson, S. Belongie, H. Greenspan, J. Malik, Blobworld: color and texture-based image segmentation using EM and its application to image querying

and classification, IEEE Trans. Pattern Anal. Mach. Intell. 24 (8) (2002) 1026–1038.
[8] V. Boskovitz, H. Guterman, An adaptive neuro fuzzy system for automatic image segmentation and edge detection, IEEE Trans. Fuzzy Syst. 10 (2) (2002) 247–262.
[9] Z. Tu, S.C. Zhu, Image segmentation by data-driven Markov Chain Monte Carlo, IEEE Trans. Pattern Anal. Mach. Intell. 24 (5) (2002) 657–673.
[10] J.K. Udupa, P.K. Saha, R.A. Lotufo, Relative fuzzy connectedness and object definition: theory, algorithms and application in image segmentation, IEEE Trans. Pattern Anal. Mach. Intell. 24 (11) (2002) 1485–1500.
[11] H.D. Cheng, X.H. Jiang, Y. Sun, J.L. Wang, Color image segmentation: advances and prospects, Pattern Recognition 34 (12) (2001) 2259–2281.
[12] Y. Deng, B.S. Manjunath, Unsupervised segmentation of color-texture regions in images and video, IEEE Trans. Pattern Anal. Mach. Intell. 23 (8) (2001) 800–810.
[13] M. Mirmehdi, M. Petrou, Segmentation of color textures, IEEE Trans. Pattern Anal. Mach. Intell. 22 (2) (2000) 142–159.
[14] J. Shi, J. Malik, Normalized cuts and image segmentation, IEEE Trans. Pattern Anal. Mach. Intell. 22 (8) (2000) 888–905.
[15] Y. Zhang, A survey on evaluation methods for image segmentation, Pattern Recognition 29 (8) (1996) 1335–1346.
[16] L. Shafarenko, M. Petrou, J. Kittler, Automatic watershed segmentation of randomly textured color images, IEEE Trans. Image Process. 6 (11) (1997) 1530–1544.
[17] E. Littman, H. Ritter, Adaptive color segmentation – a comparison of neural and statistical methods, IEEE Trans. Neural Network 8 (1) (1997) 175–185.
[18] P. Campadelli, D. Medici, R. Schettini, Color image segmentation using Hopfield networks, Image Vis. Comput. 15 (3) (1997) 161–166.
[19] A. Verikas, K. Malmqvist, L. Bergman, Color image segmentation by modular neural network, Pattern Recognition Lett. 18 (2) (1997) 173–185.
[20] D.K. Panjwani, G. Healey, Markov random field models for unsupervised segmentation of randomly textured color images, IEEE Trans. Pattern Anal. Mach. Intell. 17 (10) (1995) 939–954.
[21] K. Haris, S.N. Efstratiadis, N. Maglaveras, A.K. Katsaggelos, Hybrid image segmentation using watershed and fast region merging, IEEE Trans. Image Process. 7 (12) (1998) 1684–1699.
[22] T. Uchiyama, M.A. Arbib, Color image segmentation using competitive learning, IEEE Trans. Pattern Anal. Mach. Intell. 16 (12) (1994) 1197–1206.
[23] C.L. Huang, Parallel image segmentation using modified Hopfield model, Pattern Recognition Lett. 13 (5) (1993) 345–353.
[24] L. Lucchese, S.K. Mitra, Color image segmentation: a state of the art survey, in: Proceedings of the Indian National Science Academy on Image Processing, Vis. Pattern Recognition 67 (2) (2001) 207–221.
[25] P.K. Loo, C.L. Tan, Adaptive region growing color segmentation for text using irregular pyramid, in: 6th International Workshop on Document Analysis Systems, vol. 3163, 2004, pp. 264–275.
[26] Z. Yu, O.C. Au, R. Zou, W. Yu, J. Tian, An adaptive unsupervised approach toward pixel clustering and color image segmentation, Pattern Recognition 43 (5) (2010) 1889–1906.
[27] R.C. Gonzalez, R.E. Woods, in: Digital Image Processing, Prentice Hall, Englewood Cliffs, NJ, 2002.
[28] A.K. Jain, in: Fundamentals of Digital Image Processing, Prentice Hall, Upper Saddle River, NJ, 1989.
[29] P.K. Sahoo, S. Soltani, A survey of thresholding techniques, Comput. Vis. Graphics Image Process. 41 (2) (1988) 233–260.
[30] D.C. Tseng, C.H. Chang, Color segmentation using perceptual attributes, IEEE Int. Conf. Image Process. 3 (1992) 228–231.
[31] H. Cheng, Y. Sun, A hierarchical approach to color image segmentation using homogeneity, IEEE Trans. Image Process. 9 (12) (2000) 2071–2082.
[32] J.C. Dunn, A fuzzy relative of the ISODATA process and its use in detecting compact, well separated cluster, Cybernetics 3 (3) (1973) 32–57.
[33] J.C. Bezdek, in: Pattern Recognition with Fuzzy Objective Function Algorithms, Plenum Press, New York, 1981.
[34] S.S. Reddi, S.F. Rudin, H.R. Keshavan, An optimal multiple threshold scheme for image segmentation, IEEE Trans. Syst. Man Cybernet. 14 (4) (1984) 661–665.
[35] J.C. Bezdek, Cluster validity with fuzzy sets, Cybernet. Syst. 3 (3) (1974) 58–73.
[36] N.R. Pal, J.C. Bezdek, On cluster validity for the fuzzy c-means model, IEEE Trans. Fuzzy Syst. 3 (3) (1995) 370–379.
[37] X.L. Xie, G.A. Beni, Validity measure for fuzzy clustering, IEEE Trans. Pattern Anal. Mach. Intell. 13 (4) (1991) 841–847.
[38] J. Liu, Y.H. Yang, Multiresolution color image segmentation, IEEE Trans. Pattern Anal. Mach. Intell. 16 (7) (1994) 689–700.
[39] M. Borsotti, P. Campadelli, R. Schettini, Quantitative evaluation of color image segmentation results, Pattern Recognition Lett. 19 (8) (1998) 741–747.

Khang Siang Tan received his B.Eng. degree in Mechatronic Engineering from Universiti Sains Malaysia (USM), Malaysia in the year 2009. He is currently pursuing his M.Sc. degree in Electrical and Electronic Engineering and is attached to the Imaging and Intelligent Systems Research Team (ISRT), School of Electrical and Electronic Engineering, USM. His research interests include image enhancement and image segmentation.

Nor Ashidi Mat Isa received the B.Eng. degree in Electrical and Electronic Engineering with First Class Honors from USM in 1999. In 2003, he went on to receive his Ph.D. degree in Electronic Engineering (majoring in Image Processing and Artificial Neural Network). He is currently an Associate Professor and lecturing at the School of Electrical and Electronic Engineering, USM. His research interests include intelligent systems, image processing, neural network, biomedical engineering, intelligent diagnostic systems and algorithms. As of now, he has led his ISRT research group to publish at both national and international arena. Their contributions can be found in numerous journals, chapters in books and proceedings.